## POLITECNICO DI TORINO
## Repository ISTITUZIONALE

Damage of repeatedly nitrocarburised steel dies for aluminium extrusion

(Article begins on next page)

25 April 2024

# Damage of repeatedly nitrocarburized steel dies for aluminium extrusion

P.Matteis[1]*, G. Scavino[2], E. Quadrini[3], P. Perucci[4], D. Firrao[5].

[1] DISMIC, Politecnico di Torino, Corso Duca degli Abruzzi 24, It-10129, Torino, Italy. Tel. +390115644711, Fax +390115644699, paolo.matteis@polito.it

[2] DISMIC, Politecnico di Torino, Corso Duca degli Abruzzi 24, It-10129, Torino, Italy. Tel. +390115644675, Fax +390115644699, giorgio.scavino@polito.it

[3] Dip. Meccanica, Università Politecnica delle Marche, Via Brecce Bianche 1, It-62029, Ancona, Italy. Tel. +390712204731, e.quadrini@univpm.it

[4] Via Enrico Sparapani 171, It-60131, Ancona, Italy. Tel. +393294186184, paoloperucci@hotmail.it

[5] DISMIC, Politecnico di Torino, Corso Duca degli Abruzzi 24, It-10129, Torino, Italy. Tel. +390115644663 or +390115646356, Fax +390115644699, donato.firrao@polito.it

* Corresponding author

# Abstract

The dies employed for the hot extrusion of aluminium alloys are subjected to repeated cycles of nitriding, or nitrocarburizing, after service periods of given length. Three dies, fabricated with ISO X40CrMoV5-1 (AISI H13) steel and liquid nitrocarburized, were examined either in the as-fabricated condition, or after one service period, or after 12 nitrocarburizing and service cycles (end of life). Samples cut from the die subjected to one service period were re-nitrocarburized with increasing durations and similarly examined. The examination methods included X-ray diffraction, metallography, microhardness profile measurements, and SEM fractography. The service temperature induced microstructural modifications in the core and in the case. Microcracks and wear craters, due to adhesive wear, occurred at the bearing surfaces. The wear mechanisms at the bearing surface, the microstructural evolution close to the same surface, the fatigue crack nucleation and early growth, and their interrelations and consequences during the whole die life, are discussed.

# Keywords

# Introduction

In industrial practice, hot extrusion of aluminium alloys is commonly performed without lubricating the die-aluminium interface, and by using either flat-faced dies (for solid sections) or hollow dies with flat shear faces[1]. The dies are subjected both to wear upon their bearing surfaces and to mechanical and thermal fatigue, each extruded billet yielding one cycle (press cycle). The billet and die average temperatures are usually kept in the 450 to 500 °C range[2-4], and the extrudate exit temperature in the 500 to 560 °C range[5], but the local extrudate and tool temperatures at the bearing surface can be up to 580 °C[6].

The dies are usually fabricated using quenched and tempered ISO X40CrMoV5-17 (or AISI H13, Table 1) tool steel and are surface treated to improve their wear resistance. The recommended massive heat treatment consists of austenitizing at about 1025 °C, quenching, and double tempering in the 550 to 650 °C temperature range[7-9]. The recently introduced duplex surface treatments (consisting of a PVD coating upon a nitrided layer) yield the longest tool lives[3,4,10,11], but their use is limited by their higher cost and by the difficulty of the PVD process to coat the deep and narrow cavities used to extrude thin-walled sections[2,4]. Only plain nitriding or nitrocarburizing treatments, not affected by this limitation, are discussed here.

Nitriding or nitrocarburizing generally cause at the surface of steels the formation of a thin top layer (also known as white layer or, less preferable, compound layer), where nitrides and carbonitrides of the $\gamma$'-Fe$_4$N or $\varepsilon$-Fe$_{2-3}$(C,N) types predominate, followed by a thicker N diffusion layer[12-19]. In the current practice, the total nitriding depth of the aluminium extrusion dies is usually chosen in the 100 to 300 µm range, and a 5 to 15 µm thick top layer is present in most cases[19,2]. Nitrocarburizing (rather than merely nitriding) is used to increase the $\varepsilon$ phase C content and its fraction in the top layer, and thus the surface hardness and toughness[12,15-16], whereas the substrate below the top layer is not significantly enriched of C[17]. The microstructure of the N diffusion layer was investigated in several gas-nitrided alloy steels[20-24] and ion-nitrided tool steels

(including X40CrMoV5-1)[25], containing about 3 or 5% Cr, with a tempered martensite original microstructure. In all these cases, the diffusion layer consists of the original C saturated ferrite matrix, further saturated with N up to 0.1%[26], finely dotted by alloy-element nitride precipitates which raise the hardness. Furthermore, C is displaced by N in previous carbides thus converted to nitrides[20,21,24,25]. The nitride precipitates are mainly CrN in the X40CrMoV5-1 case[25], but mixed alloy nitrides with Mo, V, and Fe, generally isomorphous to CrN, may also occur[24]. Moreover, detailed examinations of the gas-nitrided alloy steels assessed that: i) the fine intralath Cr-rich carbides are dissolved[20,21]; ii) the coarser lath-boundary Cr-rich carbides[20,21], as well as other mixed alloy carbides and V carbides[24], are slowly replaced *in-situ* by nitrides; iii) the displaced C atoms re-precipitate as cementite ($Fe_3C$) at previous austenitic grain boundaries parallel to the stress field[20-23]. The shape of the N concentration vs. depth profile depends upon the competition between the N diffusion and the nitride precipitation, the former favouring a continuously decreasing profile, and the latter a steep profile whose high value depends from the amount of available nitride-forming alloy elements[27,28]. An intermediate profile, consisting of an initial plateau (similarly determined by the steel composition) followed by a gradual decrease, occurs upon gas-nitriding Cr-alloyed steels[24,27]. In these latter cases, aging, at a temperature close to the nitriding one, induces only a limited inward N diffusion[24], because most N atoms are bound into the precipitates[21].

The die service life consists of repeated stages, each comprising a nitriding (or nitrocarburizing) treatment and a production run[4], but may also include trial production runs, repairs, and shape corrections. Repairs can be performed by manually polishing (with emery paper) some severely worn areas, as long as the extrudate dimensional allowances (usually comprised in the 0.15 to 0.30 mm range) can be met. Shape corrections can be performed by electrical-discharge or mechanical machining. Both repairs and shape corrections are followed by a surface treatment. Thus successive surface treatments can be performed either on previously treated and worn surfaces, with different local damage levels, or on newly polished or machined ones.

The most common die failure modes are mechanical fatigue fractures (often with different cracks initiating at distant locations), wear, and deflection (creep-like plastic deformation), leading to increasing, and finally unacceptable, extrudate size, shape or roughness defects[29]. Moreover, thermal fatigue in hot working applications results in networks of surface cracks referred to as *heat checking*.

The wear mechanisms occurring in service at the nitrided bearing surface have been studied either after actual production runs[2-5,8] or by using specific wear tests[3,7], and are shortly reviewed hereafter. The contact pressure between the extrudate and the tool is maximum at the bearing inlet and decreases toward the bearing outlet. Thus, at the bearing inlet the aluminium adheres to the tool surface and is only discontinuously renewed (the extrusion occurs by shear inside the aluminium), whereas at the bearing outlet the extrudate slides continuously upon the tool surface[2-4]; the actual extensions of these inlet and outlet region, and of the transition region between them, varies widely among different press and tool setups. The chemical wear, due to the diffusion of tool elements in the extrudate, occurs continuously in the transition region[3], whereas elsewhere it is hindered either by the slow aluminium renewal (inlet region) or by a less intimate contact between the extrudate and the tool (outlet region)[30]. The adhesive wear is mainly related to the extrusion interruptions occurring at each press cycle, while the new billet is introduced: chemical bonds (i.e. new Fe-Al-Mg-O phases)[4] are developed at the interface between the aluminium and the tool during these interruption, and then lead to micro-fractures at the tool surface, leaving discrete craters 20 to 100 μm deep[3]. Because the die fracture strength is much higher than the extrudate shear strength, a fatigue mechanism has been hypothesized for the nucleation and propagation of microcracks at the nitrided tool surface, prior to the detachment of the wear fragments[4]. Thereafter, the wear craters depth increases linearly with the number of press cycles[5], the exposed substrate being progressively worn.

The usefulness of the top layer is debated[2,4]; according to Kugler et al.[2], a thin monophasic (tough) top layer (formed only by high C ε phase)[16] can improve the wear resistance, due to its higher

chemical stability against hot aluminium (in respect to the diffusion layer) and to its lower friction coefficient, whereas a thick biphasic (brittle) one (formed by both γ' and ε) can favour the formation of surface microcracks (spalling).

The resistance to mechanical fatigue and fracture of nitrocarburized dies having been extensively studied elsewhere[16], the present work examines the influence of the repeated nitrocarburizing and service stages on the microstructure/property evolution and wear damage of the extrusion dies

## Experimental procedures

Three multi-hole dies, fabricated with ISO X40CrMoV5-1 tool steel[*], were examined.

The A die was never used and it was examined after the first nitrocarburizing. The B die was a one-piece flat-face die yielding two equal solid extrudates, whereas the C bridge die was a cap-and-mandrel assembly yielding two equal semihollow extrudates (Fig. 1); their service and nitrocarburizing schedules are reported in Table 2 and 3, respectively. The B die was used to extrude 5 billets in a trial run in the as-machined condition, nitrocarburized, and used for one production run of 23 billets (1058 kg) of 6060 aluminium alloy (Table 4); then it was taken out of production and examined. The C die was examined after its whole work life, during which it was used to extrude 1060 billets (48760 kg) of 6060 aluminium alloy and was nitrocarburized 12 times (some of them after shape corrections); the mean number of press cycles between successive nitrocarburizing treatments was 75, with a large dispersion (standard deviation: 32), whereas 155 press cycles were performed after the last nitrocarburizing stage; the die was finally withdrawn from service due to the development of mechanical fatigue cracks. The total wear lengths were 2 and 50 km, respectively, for the B and C dies (Table 2 and 3). The extrusion speed was of the order of 1 m/s, and the manual billet exchanges required about 1 min each. The production rate of the C die was recorded during a 4.4 h production test, allowing to conclude that the C die mean press cycle duration was 2.4 min, and that its total service time was about 41 h (Table 3).

---

[*] Supplied by Uddeholm with the Orvar proprietary name.

All the die liquid nitrocarburizing treatments were performed by using an aerated low-cyanide sulphur-bearing salt bath[*] (Table 5)[12,14,17,32,33], for a 90 min duration, at $570 \pm 5$ °C, preceded by a 1 h pre-heating stage at 400 °C and followed by oil cooling and sandblasting.

The dies were pre-heated to 450 °C for 4 h (or more) before each service stage, the initial (homogeneous) billet temperature being in the 450 to 470 °C range, and the typical extrudate exit temperature at about 500 °C.

The bearing surface of the B die (not subjected to chemical aluminium removal) and a crack surface of the C die were examined by scanning electron microscopy (SEM); the latter crack had been opened by die sectioning. Samples representative of the bearing surfaces of all the examined dies were cut, mounted, polished, and characterized upon surfaces normal to the bearing surface, both by 300 g Vickers microhardness profiles[†], and by metallographic techniques, using either the Cogne[‡] or Nital[34] etch. The nitrocarburized surface of the A die was studied by X-ray diffraction[§] in order to determine the phase constitution of the top layer.

Furthermore, samples cut from the B die were re-nitrocarburized with the same above described method, but for 9 different durations, from 10 to 90 min, and examined with similar metallographic and microhardness testing methods.

## Results and discussion

*Microstructural evolution*

The substrate microstructure (as evaluated several millimetres below the nitrided case) was tempered martensite in all cases, with partially evident previous austenitic grain boundaries, (Fig.2). The substrate hardness was 561 and 543 HV respectively, in the A and B dies, corresponding to a 4 hour temper at approximately 570-580 °C[7,8,35], whereas it was 441 HV in the C die, tested at the

---

[*] Supplied by H.E.F. with the SurSulf proprietary name.
[†] Indentations performed along a zigzag path.
[‡] Recipe: 6 ml acetic acid, 10 ml hydrochloric acid, 1g picric acid, 100 ml ethanol; etching time: 10 s.
[§] Bragg-Brentano setup, 20° to 90° 2θ angular range, 0.02° angular steps, 8 s counting time per step, Cu $K_\alpha$ radiation to minimize penetration in a Fe-base matrix.

end of the entire service life. Thus the dies' bulk microstructure undergoes a sensible softening due to the long exposure at the service temperatures, as foreseen on the basis of a much larger Hollomon-Jaffe parameter[36]; this softening is consistent with previous results, obtained from microstructural examinations[37], softening tests[8,9], and actual dies[5].

The maximum measured case hardness was 976, 894 and 918 HV, respectively, in the A, B and C dies (at about 35 μm from the surface). A white top surface layer, of the order of 10 μm thick (Fig. 3), was evidenced by the metallographic examination at the nitrocarburized bearing surfaces of the dies A and B. Consistently with the employed nitrocarburizing process[12,14,17], the top layer consisted almost completely of the ε phase ( Fig. 4). Overall, the as-fabricated maximum case hardness and top layer structure and thickness are compatible with those previously observed in the same steel after liquid nitriding[3] or nitrocarburizing[13] processes.

The diffusion layer depth observed in the metallographic cross-sections (Fig. 3) was about 75 and 100 μm, respectively, in the A and B dies, but it was much larger in the C die. The effective depth, defined as the depth where hardness is 100 HV units higher than at core[38], was 458 μm in the C die, as opposed to 124 and 118 μm, respectively, in the A and B dies (Fig. 5). Thus, the well-known square root proportionality[25,27] is substantially respected, the case depth ratio of the as-fabricated and end-of-life dies being 3.69 (458 μm / 124 μm), only slightly higher than the square root ratio of their cumulated nitrocarburizing times (i.e. of their numbers of equal-duration nitrocarburizing stages), that was 3.46 ($\sqrt{12}$). It is inferred that, after each nitrocarburizing stage, the observable case depth depends upon the cumulated nitrocarburizing time, notwithstanding the intermediate service time.

Because the die tempering, nitrocarburizing, and service temperatures are expectedly close one to the other (at least near the bearing surface as it regards the service temperature), a microstructural evolution can be foreseen during the die service stages, not only in the substrate (as noted above), but also in the nitrided case. The substantial constancy of the metallographic case depth and of the microhardness profile shape (Fig. 5) before and after the first service stage (A and B dies) implies

that the inward in-service N diffusion was modest and consistent with previous results[24], probably because most N atoms were bound in alloy-element nitrides[21,26], and the inward diffusion of those dissolved in the matrix was hindered by the competition with nitride-precipitation phenomena (discussed below). Nevertheless, grain boundary precipitates, either parallel or at small angles in respect to the surface, were observed in the diffusion layers of the B and C dies, but not in the as-fabricated A die ( Fig. 3), and the B die hardness profile was 30 to 80 HV units lower than the A die one throughout the diffusion layer (Fig. 5).

By comparison with the previous results obtained upon gas-nitrided alloy steels[20-23], and by taking into account the preferential orientation, the precipitates parallel to the surface are recognized as cementite. Since the intergranular cementite precipitation is due to the slow transformation of the coarser alloy carbides and is slower than the intragranular CrN precipitation[20,21], and since the present liquid nitrocarburizing process is much shorter than the previously examined gas nitriding ones (lasting up to 96 h)[20], it is inferred that the cementite precipitation did not reach an observable extent during the nitrocarburizing treatment, but rather only afterward in service. The N atoms that, during the service stage, displaced the C atoms from the original alloy carbides (allowing them to re-precipitate at the grain boundaries) may have come either from less stable nitrides, or from the ferritic matrix, or both. The first hypothesis stems from the previous observation that, during a 48 h aging, mixed $Cr_xFe_{1-x}N$ nitrides reverted to CrN, allowing the excess N atoms to diffuse through the matrix and react with Cr atoms available elsewhere[24], whereas the second hypothesis stems from the previous observation that the ferritic matrix can be supersaturated in N, due to the strains arising from the coherent precipitates[21]. This second hypothesis is consistent with the homogeneous hardness decrease observed contemporaneously (after one service stage, Fig. 5) in the diffusion layer, and is more acceptable on thermodynamic bases[38]. A further, probably more important, contribution to the same case hardness decrease may have arisen from the coarsening of the intragranular CrN precipitates and from their coherent-to-incoherent transformation[21]; this latter

phenomenon can have itself contributed to the release of excess N from the matrix, by relieving the abovementioned matrix strain.

The present results imply that the duration of a production stage (consisting of 23 press cycles only) was sufficient to yield an extended cementite precipitation, whereas the further cumulated nitrocarburizing and service time did not observably increased the cementite volume fraction (as observed in the C die); therefore, the cementite precipitation was probably complete after the first production stage. Since the successive nitrocarburizing treatments increased the diffusion layer depth, each service stage probably allowed the cementite to precipitate analogously in the additional nitrided layer due to the last nitrocarburizing stage, as confirmed by the observations of the end-of-life die.

Moreover, the maximum diffusion-layer hardness at end-of-life is more than 250 HV units lower than that achieved after the 90 min re-nitrocarburizing test. Therefore, the abovementioned service aging becomes more and more pronounced during the successive service stages, and the hardening efficacy of the successive nitrocarburizing stages decreases. The latter hypothesis is justified by considering that the maximum hardness achieved in the diffusion layer is due to the fine intragranular alloy nitride precipitation, that is limited by the alloy element availability in the ferritic matrix (and in the finer carbides): in a point, once the most effective available alloy element (Cr in the present case) has been employed in the precipitation process, the hardening efficacy of the further nitrocarburizing time should decrease, while the existing fine nitride precipitates can progressively age in service. Moreover, this latter hypothesis can justify the comparatively smaller hardness gradient observed in the closer-to-surface part of the nitrided case at end-of-life (Fig. 5). In fact, the hardness gradient in the A and B dies was about 3.7 and 3.0 HV/µm, respectively, between the surface and the effective depth, whereas in the C die it was about 0.4 HV/µm between the surface and 285 µm depth, and about 1.7 HV/µm between 285 and 485 µm depth. The latter gradient transition (at 285 µm depth) may correspond to the transition from an outer region, where the more effective nitride-forming elements are almost completely precipitated into nitrides and the

hardness gradient is due to less effective mechanisms (other alloy-element precipitates, or interstitial hardening by solute N), to an inner region, where the more effective nitride-forming elements are still available and the hardness gradient is determined by the gradient of the amount of fine nitride precipitates. This latter hypothesized end-of-life N concentration profile is consistent with the previously described gas-nitriding kinetics of Cr alloyed steels[26] and with previously observed gas-nitriding concentration profiles[24].

*Wear and fatigue*

The comparison of the metallographic cross sections reported in Fig. 3 show that the homogeneous wear of the top layer was negligible after 23 press cycles in the once-used die, but it was sufficient to completely remove the top layer from the bearing surface of the end-of-life die, probably because the last service stage of the latter die was much longer (155 press cycles).

Because the nitrocarburized case is much harder than the extrudate, this homogeneous wear is probably related to the abovementioned chemical wear mechanism, rather than to an abrasive one. Moreover, the abovementioned fair agreement between case depth and square-root nitrocarburizing time implies that even at end-of-life the material loss due to the homogeneous wear was small in respect to the case depth; thus the previously noted chemical stability of the top layer[2] is confirmed.

Microcracks connected with the bearing surface were evident in metallographic cross-sections (Fig. 3C and 6C) and in some cases nitrides and carbonitrides had been formed at the microcrack surfaces (Fig. 6C). Although these compounds may initially provide a form of beneficial crack closure, their comparative brittleness (in respect to the surrounding steel) probably enhance the crack propagation rate until the crack tip overcomes the transformed region; thus, the net effect of each re-nitrocarburizing stage upon the overall growth of the fatigue microcracks is uncertain, but probably small.

The bearing surface after service, as observed in the B die, presented discrete (inhomogeneous) wear craters (Fig. 6B and 7), typically 15 to 30 μm deep (as evaluated either optically, Fig. 6B, or

from the microhardness profile offset, Fig. 5), which prevalently occurred close to the bearing inlet (Fig. 7a,b). This distribution is consistent with the abovementioned adhesive wear mechanism, because in the inlet region, as opposed to the outlet one, the contact between the aluminium and the tool is characterized by a higher pressure (directly due to the extrusion forces, or residual during the extrusion interruptions) and by the absence of the oxide layer developed further on upon the aluminium surface. Moreover, the inner surface of the wear craters (Fig. 7c,d) showed microvoids, whereas the bearing surface outside them was comparatively smooth (Fig. 7c). This fact and the observation of several surface microcracks with different lengths confirm that the wear craters arose from discrete fracture events, occurring when a fatigue microcrack reaches a critical size.

Several macroscopic fatigue cracks were developed in the smaller bridges of the C mandrel, within macroscopic plastic zones showing parallel surface marks (Fig. 8). Because the number of press cycles in a die life is of the order of $10^3$ only, these cracks pertain to the domain of low-cycle fatigue, and occurred by large advancements.

Some cracks started from bridge surfaces faced to extrusion dead metal zones at the mandrel's inlet (Fig. 8a,b), and showed a plastic zone extended trough the whole bridge thickness (Fig. 8b) corresponding to generalized yielding of the bridge, thus not only the fatigue cracks reduced the mandrel stiffness, but also the bridge plastic deformation contributed to deteriorate the mandrel shape, and ultimately both contributed to critically modify the extrudate geometry.

A macroscopic spalling area close to the abovementioned plastic zone (Fig. 8b) may have been induced by the inability of the nitrided case to deform with the substrate.

Other cracks started at the mandrel's outlet (Fig. 8c) and showed a serrated path with steps dictated by surface marks (Fig. 8c,d).Moreover, the not oxidized (inner) part of the examined crack surface presented large striations (Fig. 8e,f), consisting of alternated tearing and shear regions (Fig. 8f). This allows to hypothesize that the crack advancements occur alternatively by plastic tearing (at press-cycle starts, when the load is first applied) and by plastic shearing across or along previously formed localized shear bands, which are evidenced by the abovementioned surface marks.

*Re-nitrocarburizing tests*

Representative microhardness profiles obtained after the re-nitrocarburizing tests are shown in Fig. 9. The maximum measured diffusion layer hardness increased continuously with the re-nitrocarburizing time, from the original 894 HV to a maximum of 1204 HV after the 90 min test, while the hardness gradient was almost unaltered (Fig. 9). The case depth increase was more rapid (on the basis of the square root relationship) than observed in the die nitrocarburizing stages, perhaps because the salt bath recirculation was better around the sectioned samples than inside the narrow die bearing channel; thus, each re-nitrocarburizing test represents a somewhat longer die re-nitrocarburizing stage.

The microhardness profile below a previous wear crater, examined after the 30 min re-nitrocarburizing test, presented a larger hardness increase and a steeper hardness gradient, than below the undamaged areas (Fig. 10), the N intake being expectedly somewhat faster because surfaces free from the top layer were exposed[40,12].

Generally, the top white layer was more rapidly formed inside the microcracks (due to the previous service stage) than on the surface of the wear craters: it was already observed inside one microcrack after the 10 min test (Fig. 11a) and several similar cases where observed after longer durations (Fig. 11c); this may happen because the salt bath infiltrates the microcracks, or because they influence the N diffusion paths. Instead, some wear craters did not yet showed a continuous newly formed top layers after the 50 min re-nitrocarburation test (Fig. 11a,b); this may arise from the presence of oxides or other impurities, that, prior to re-nitrocarburizing, are not as easily removed from the rough bottom of the wear craters as from the rest of the bearing surface.

Thus, re-nitrocarburizing stages shorter than those employed would probably not be sufficient to reform the top layer, and, consequently, the formation of nitrides and carbonitrides inside the microcracks appears unavoidable in the examined industrial practice.

# Conclusions

The tool steel dies used for aluminium extrusion and repeatedly nitrocarburized are subjected to several damage mechanisms.

The service temperature affects both the quenched and tempered core and the nitrocarburizing diffusion layer. The core microstructure is softened, probably through the known prolonged tempering mechanisms. The diffusion layer is softened, probably mainly due to the overaging of the fine nitride precipitates, and subjected to cementite precipitation at prior austenitic grain boundaries. These diffusion layer modifications occur after each nitrocarburizing stage. A further damage mechanism due to the service temperature, not investigated here, is probably the relieving of the beneficial compressive stress state induced by the nitrocarburizing treatment. Overall, this suggests that the time at temperature is a relevant die damage parameter, alongside the wear length.

The wear of the bearing surfaces induces surface microcracks that then lead to wear craters. This wear mechanism probably arises from adhesive bonds formed between the tool and the extrudate during the extrusion interruptions. A further wear mechanism results in a comparatively slow homogeneous consumption of the top layer, and is probably of chemical nature.

The successive nitrocarburizing stages restore the top layer (protecting the substrate from chemical wear), and counteract the service softening of the diffusion layer, probably by forming further alloy element nitrides. The latter effects is progressively hindered (through several nitrocarburizing and service stages), probably for lack of further nitride-forming alloy atoms in the ferritic matrix. A probable, but not investigated, further effect of the re-nitrocarburizing stages may be to restore the compressive stress state; because also this effect arises from further nitride precipitation, it may also progressively decrease for lack of available alloy atoms, at least close to the surface.

The growth rate and the crack path of macroscopic cracks are driven by the overall stress state determined by the extrusion forces at each press cycles; due to the steel's large fracture toughness at the service temperature, the crack advancement occurs by fatigue by a tearing and shear

mechanism. The large plastic deformation, occurring on several localized shear bands, also contributes to the die failure (i.e. inability to yield the desired shape).

Some fatigue cracks were developed from surfaces scarcely subjected to wear damages (e.g. surfaces facing dead metal zones), that had been re-nitrocarburized although their top layer was probably unaltered. Albeit this fact in part arises from the design of the examined die, it suggests that selective re-nitrocarburizing treatments may be tried to prevent the excessive increase of the case depth in these zones.

# Acknowledgements

# References

1. F. F. Kraft and J. S. Gunasekera: in: 'ASM Handbook - Vol. 14A - Metalworking: Bulk Forming', (ed. S. L. Semiatin et al.), 421-439; 2005, Materials Park OH (USA), ASM International.

2. G. Kugler, R. Turk, T. Vecko-Pirtovsek and M. Tercelj: Metalurgija, 2006, 45 (1), 21-29.

3. T. Bjork, J. Bergstrom and S. Hogmark: Wear, 1999, 224, 216-225.

4. T. Bjork, R. Westergard and S. Hogmark: Wear, 2001, 249, 316–323.

5. P. K. Saha: Wear, 1988, 218, 179-190.

6. M. Tercelj, G. Kugler, R. Turk, P. Cvahte and P. Fajfar: Int. J. Vehicle Design, 2005, 39 (1-2), 93-109.

7. ISO 4957:1999. Tool steels.

8. ORVAR Supreme - Hot work tool steel. Uddeholm, 2005.

9. A.M. Bayer, T. Basco and L.R. Walton: in 'Metals Handbook - 10th ed. - Vol. 1 - Properties and Selection: Irons, Steels and High Performance Alloys', (ed. J.R. Davis et al.), 757-779; 1990, Materials Park OH (USA), ASM International.

10. T. Bjork, R. Westergard, S. Hogmark, J. Bergstrom and P. Hedenqvist: Wear 1999, 225-229, 1123-1130.

11. M. B. Karamis and H. Sert: Wear, 1998, 217, 46-55.

12. D. Firrao, M. Rosso and G. Scavino: Metall. Ital., 1986, 78 (4), 285-304 (in Italian).

13. Li-Ho Chiu, Chang-Hui Wu and Heng Chang: Wear 2002, 253, 778–786.

14. 'Sursulf - A nitriding treatment in a non-polluting salt bath accelerated with sulphur'; 1980, Andrezieux Boutheon (France), Hydromecanique et Frottement (H.E.F.).

15. D. Firrao and M. Rosso: Atti Acc. Sc. Torino, 1980, 114, 171-181.

16. D. Firrao and D. Ugues: Mater. Sc. Eng. A, 2005, 409, 309-316.

17. H. C. F. Rozendaal, P. F. Colijn and H. J. Mittemeijer: Proc. 'Heat treatment '84', London, UK, sep. 1984, The Metals Society, London, 1984, 31.1-31.16

18. G. N. Neustroev and V. V. Bogdanov, Metallovedenie Term. Obrabot. Metallov, 1970, 10, 45-49

19. D. Firrao, B. De Benedetti, Metall. Ital., 1976, 68, 4-14

20. S. Mridha and D. H. Jack: Metal Sc., 1982, 16, 398-404.

21. E. J. Mittemeijer: J. Metals, 1985, 37, 16-20

22. L. Barrallier, V. Traskine and S. Botchenkov: Mater. Sc. Eng. A, 2005 393, 247–253.

23. V. Y. Traskine, S. E. Bochenkov, Z. N. Skvortsova and L. Barrallier: Colloid J., 2005, 67, 97–102.

24. C. Ginter, L. Torchane, J. Dulcy, M. Gantois, A. Malchere, C. Esnouf and T. Turpin: Metall. Ital., 2006, 98 (7-8), 29-35.

25. K. Ozbaysal, O. T. Inal and A. D. Romig: Mater Sc. Eng., 1986, 78, 179-191.

26. F.K. Naumann, G. Langenscheid, Arch. Eisenhuttenw., 1965, 36, 677-682

27. B. J. Lightfoot and D. H. Jack: Proc. 'Heat Treatment 73'. London, UK, dec. 1973, The Metals Society, London,1973, 248-254.

28. A. Burdese, D. Firrao, M. Rosso, in: Proc. Heat Treatment '84, Met. Soc., London 1984, 32.1-32.7

29. A. F. M. Arif, A. K. Sheikh and S. Z. Qamar: J. Mater Process. Tech., 2003,134, 318-328.

30. M. P. Clode and T. Sheppard, Mater. Sc. Tech., 1990, 6, 755-763

31. R. B. C. Cayless: in 'Metals Handbook - 10th edition - Vol. 2: Properties and Selection: Nonferrous Alloys and Special-Purpose Materials' (ed. J. R. Davis et al.), 15-28; 1990, Materials Park OH (USA), ASM International.

32. Q. D. Mehrkam, J. R. Easterday, B. R. Payne, R. W. Foreman, D. Vukovich and A. D. Godding: in: 'ASM Handbook - Volume 4 - Heat treating', (ed. J. R. Davis et al.), 410-419; 1991, Materials Park OH (USA), ASM International.

33. D. Firrao, M. Rosso and G. Scavino. Notiziario Tecnico AMMA, 1984, 39 (5), 5-16

34. E407-99, Standard practice for microetching metals and alloys, ASTM, 1999.

35. E140-02e1. Standard hardness conversion tables for metals. ASTM, 2002.

36. J.H. Hollomon, L.D. Jaffe, Trans AIME, 1945, 162, 223-249

37. G. Cornacchia, M. Gelfi, M. Faccoli and R. Roberti: in Proc. '7th Int. Tooling Conf.', (eds. M. Rosso et al.), Torino (Italy), may 2006, Ancora, Milan (Italy), 2006, Vol. 2, 175-182.

38. UNI 5478:1999, Heat treatment of metallic materials - Nitriding, UNI, 1999

39. D. Firrao, M. Rosso, B. De Benedetti, Atti Acc. Sc. Torino, 1980, 114, 383-393

40. D. H. Jack, I. M. Stoney, Scand. J. Metall. 1 (1972) 217-221

# List of Figure Captions

Fig. 1 – Shape of the examined aluminium extrusion dies, and respective extruded sections. One-piece flat-face B die: inlet and outlet views as recomposed after sampling, view of a sample employed for the re-nitrocarburizing tests, and drawing of the extruded section (B). Mandrel and cap of the C die: inlet and outlet views and drawing of the extruded section (C).
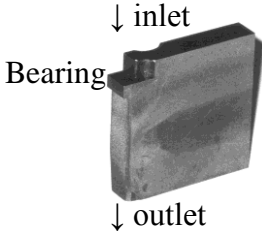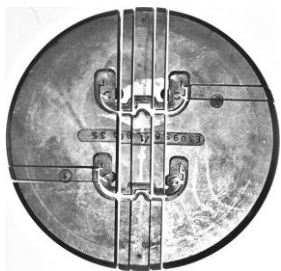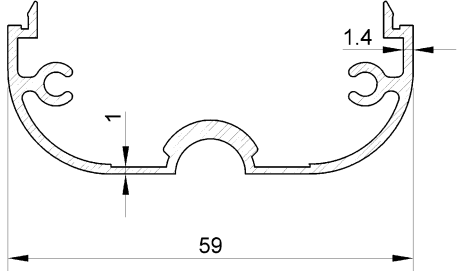
Fig. 2 – Core microstructure of the C die (tempered martensite), Cogne etch.
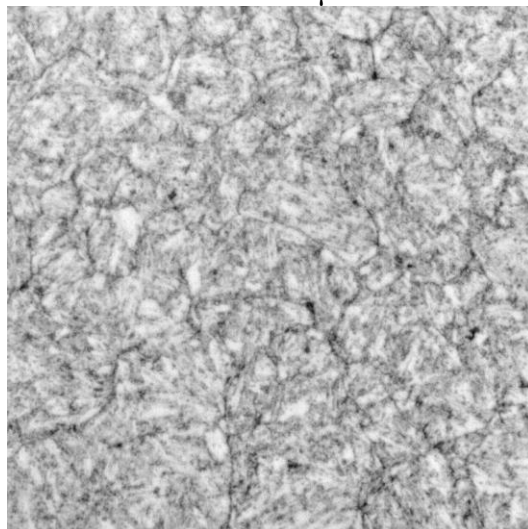
100 x 100 μm

Fig. 3 – Nitrocarburized layer at the bearing surfaces of the dies A (as fabricated and nitrided), B (after one production run), and C (at end of life). Top layer and diffusion layer in the A and B dies. Thick diffusion layer, without remaining top layer, in the C die. Grain boundary precipitates in the B and C dies. Microcrack (arrow) in the C die.
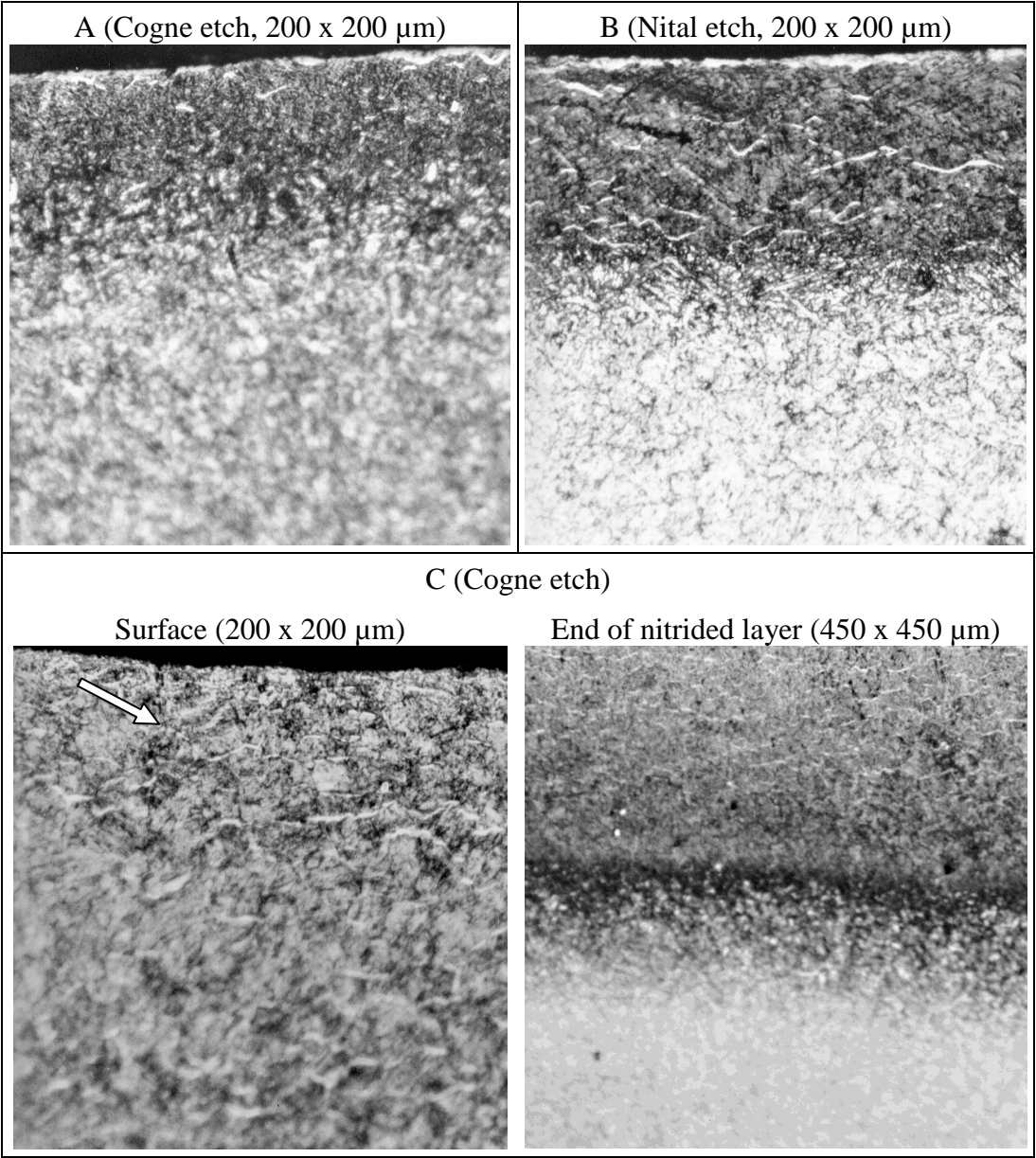


A (Cogne etch, 200 x 200 μm)

B (Nital etch, 200 x 200 μm)

C (Cogne etch)

Surface (200 x 200 μm)

End of nitrided layer (450 x 450 μm)

Fig. 4 - X-ray diffraction angular profiles of the bearing surface of the A die; theoretical diffraction angles of the ε and γ' phases.
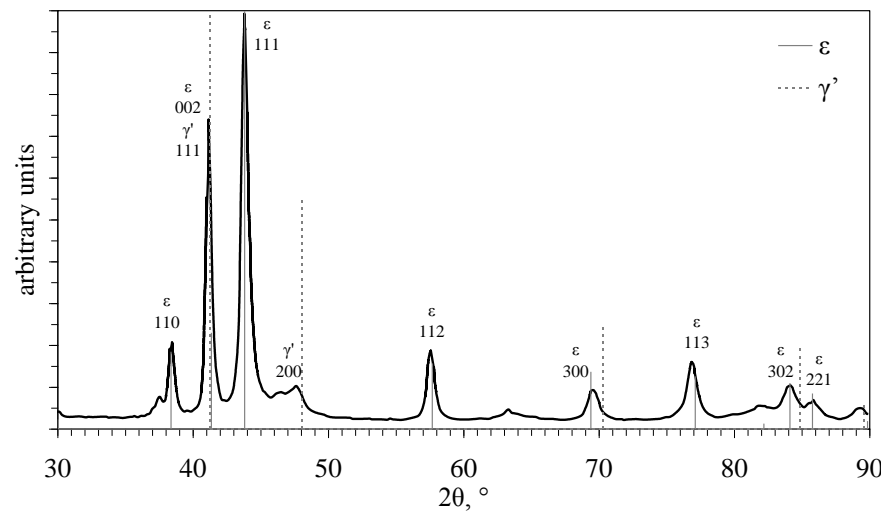


Fig. 5 – Microhardness profiles of a bearing surface of the examined dies: as fabricated and nitrocarburized (A die); after one production run, both below an undamaged area and below a wear crater (B die); at the end of the useful tool life, after repeated nitrocarburizing and production stages (C die).
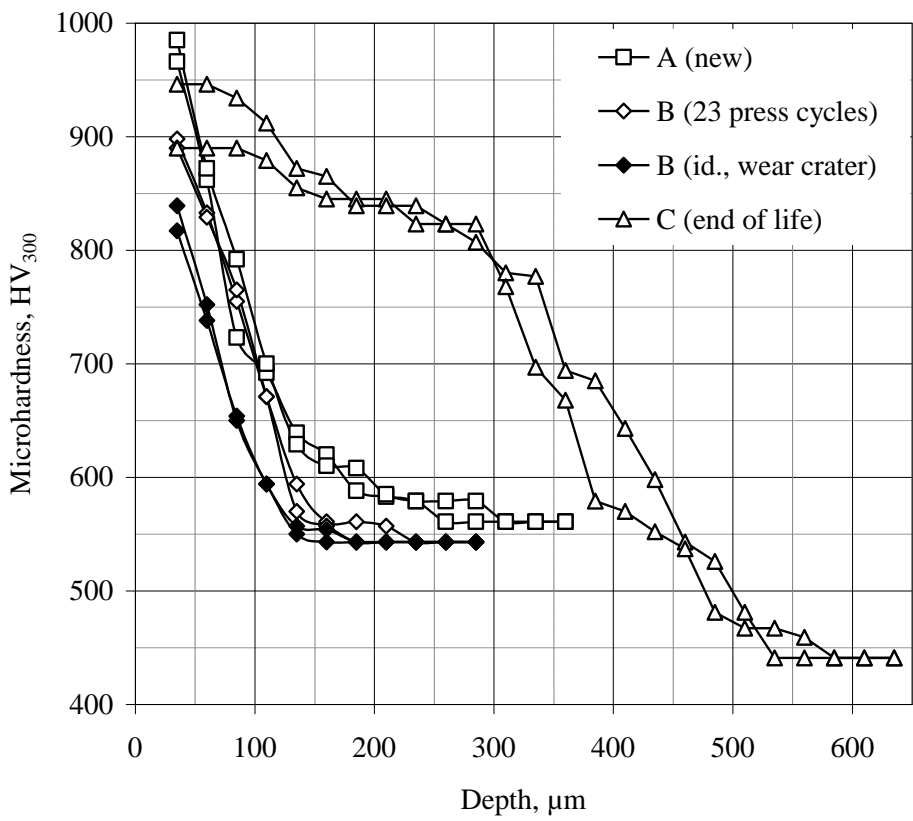
Fig. 6 - Damage mechanisms at the bearing surfaces evidenced on metallographic cross-sections. Wear crater in the B die after one production run (B). Microcracks in the C die after repeated nitrocarburizing and service stages, with white-etching regions intruding towards the interior along previously formed cracks (C).



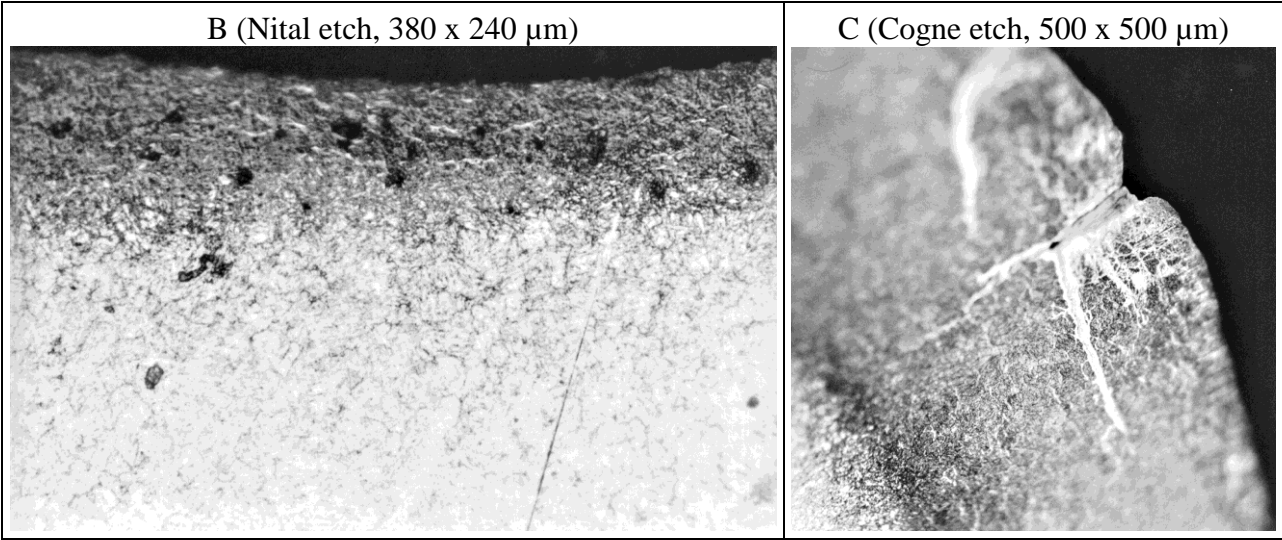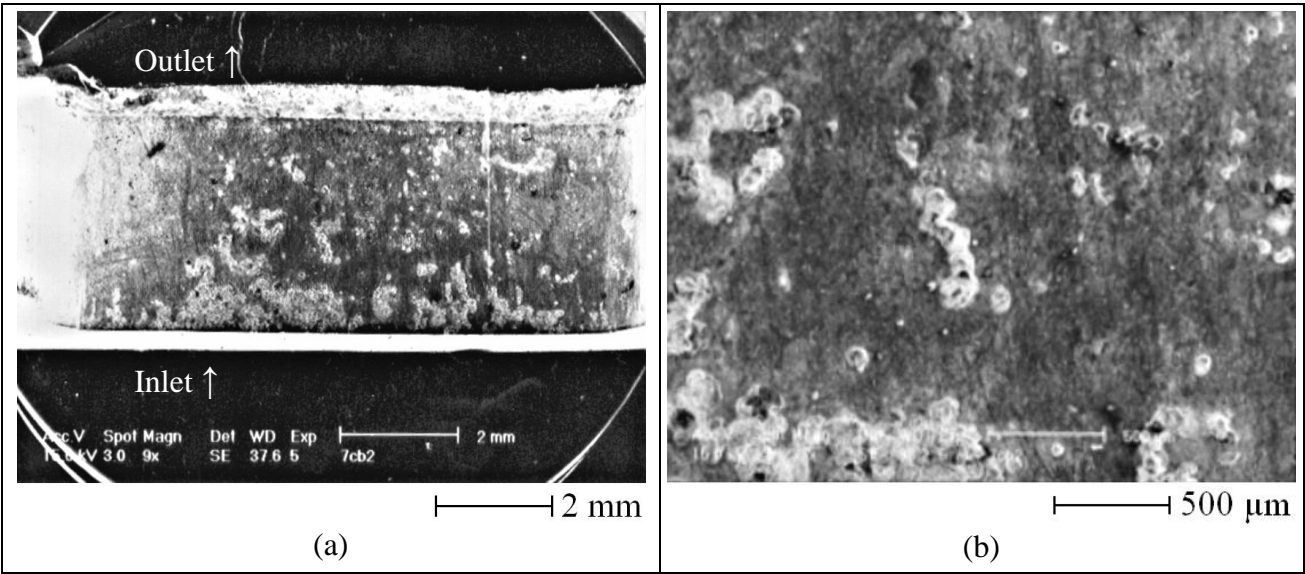| B (Nital etch, 380 x 240 μm) | C (Cogne etch, 500 x 500 μm) |

Fig. 7 – Bearing surface of the B die. Distribution of the wear craters along the bearing channel (a) and mid-point detail (b). Surface appearance of a wear crater and of the surrounding unaltered area (both cross-sectioned by a metallographic cut, c). Higher magnification of the inner surface of the same wear crater (d).
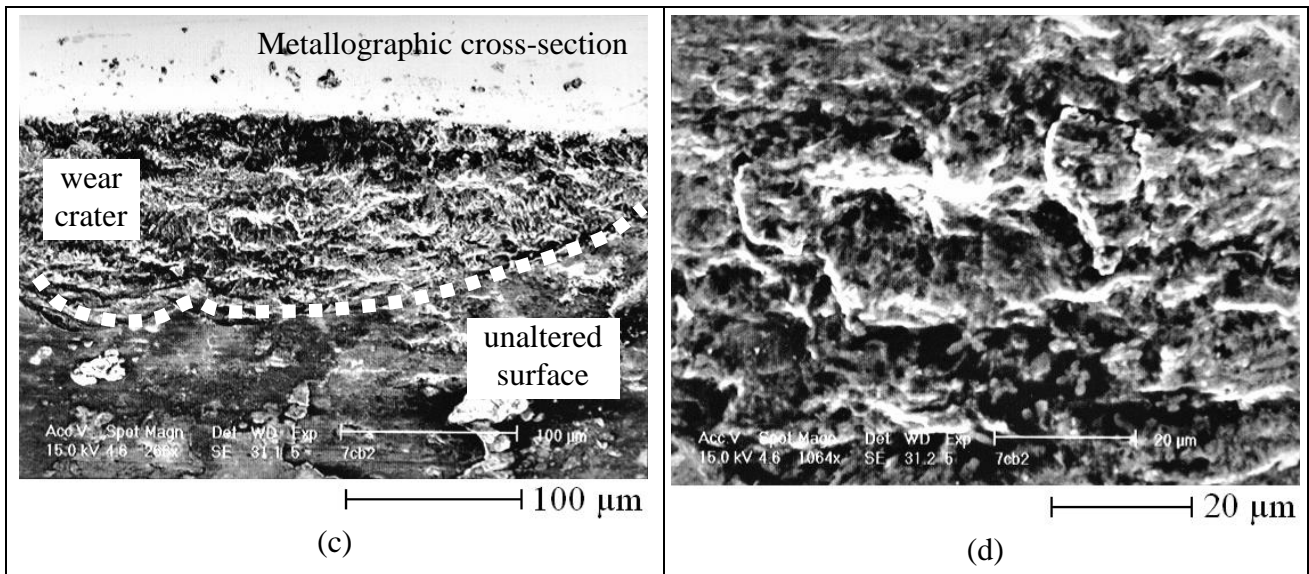
Fig. 8 – Fatigue cracks and plastic deformation surface marks at end-of-life in the smaller bridges of the C mandrel. Cracks originating from inlet dead metal zones (a,b); deformation marks extended throughout the bridge thickness (b); crack originating from the outlet extrusion welding zones (c), with surface steps of the order of 1 mm (d). Fatigue beach-marks on a crack surface (SEM, e) and detail showing alternated tearing and shear regions (f).

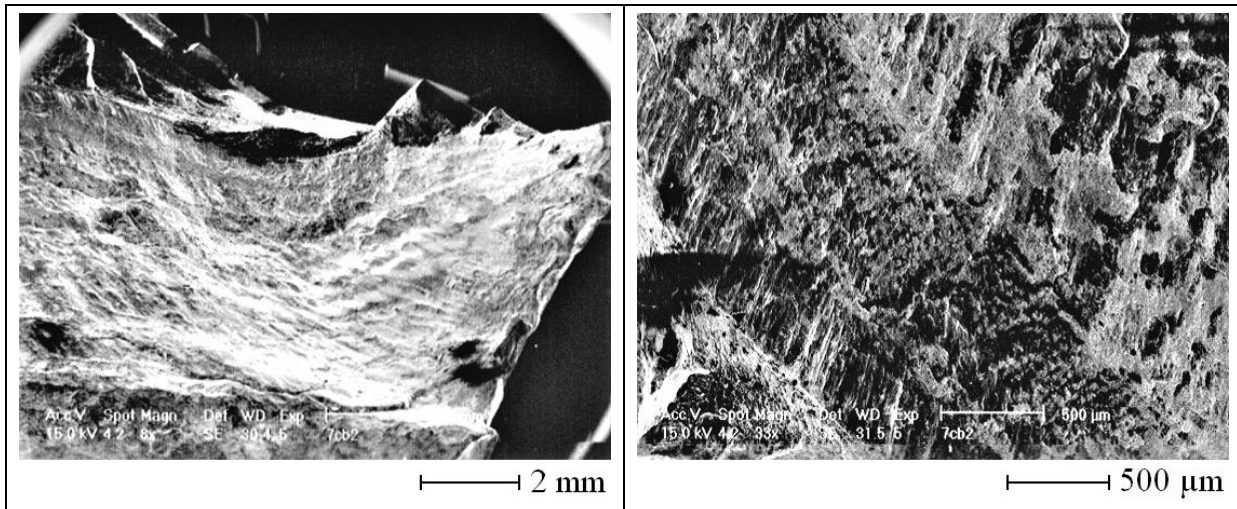├──────┤ 2 mm

├──────┤ 500 µm
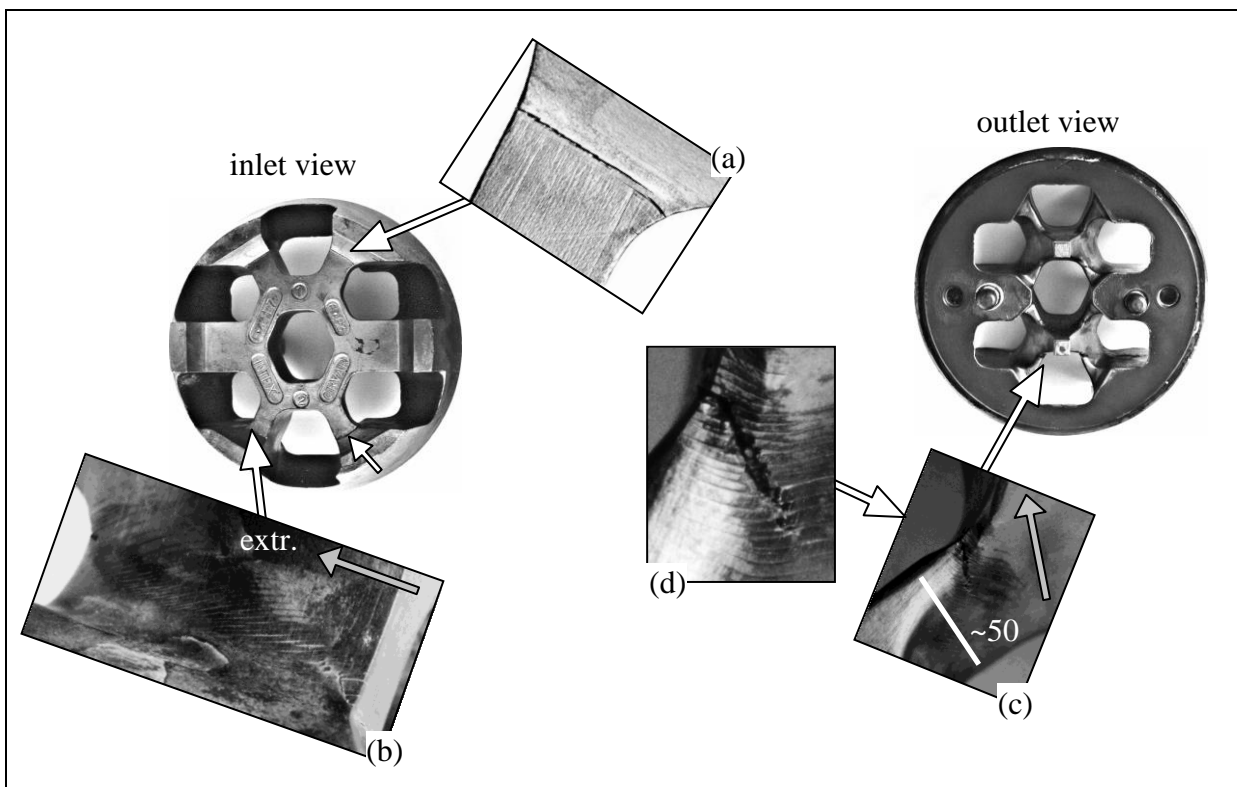
Fig. 9 - Microhardness profiles of samples taken from the B die bearing surface area, after one production run; before (0 min) and after re-nitrocarburizing tests of increasing duration.
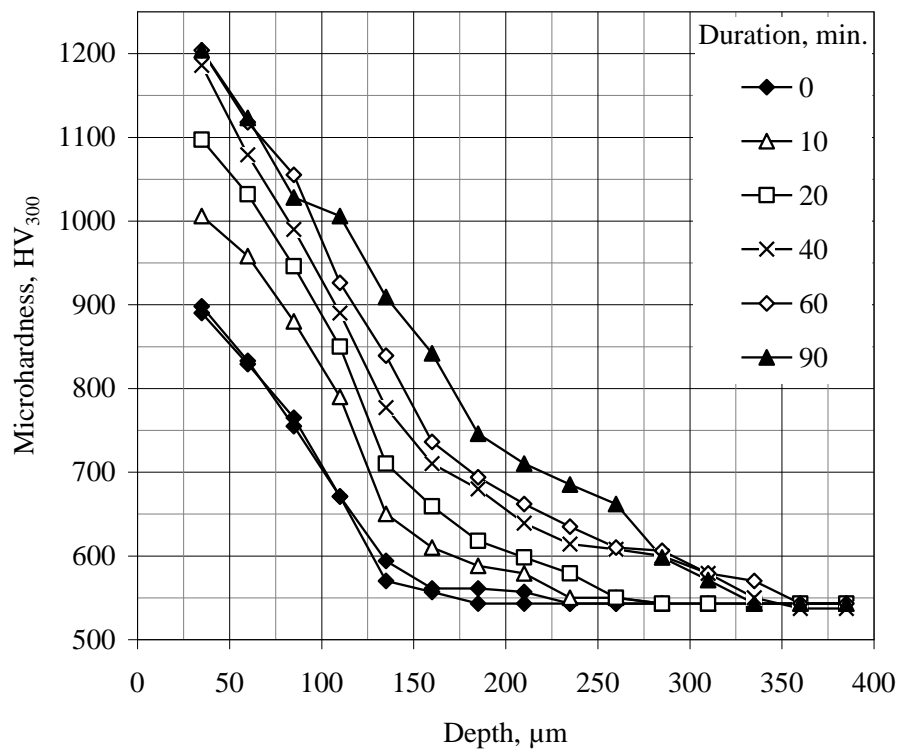
Fig. 10 - Microhardness profiles of samples taken from the B die bearing surface area, after one production run, before and after the 30 min re-nitrocarburizing test, below an undamaged area and below a wear crater.
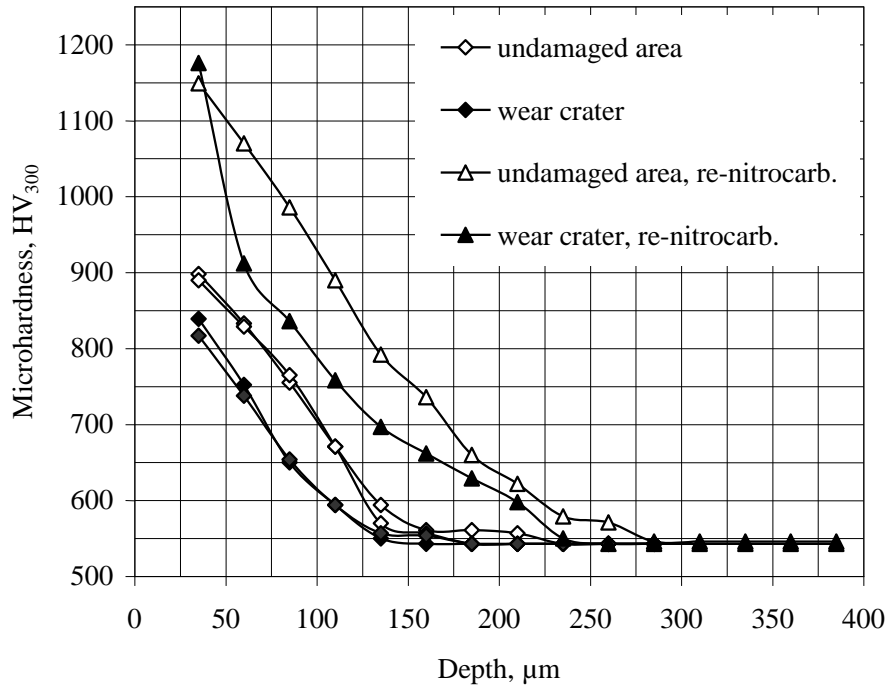


Fig. 11 - Metallographic cross-sections of the B die bearing surface, after a service stage and re-nitrocarburizing tests of increasing duration. 10 min test: white layer formed in a microcrack (a, left), but not yet on a previous wear crater (a, right). 50 min test: white layer not yet completely formed on a wear crater (b). 70 min test: evident white layer at the surface and inside the microcrack (c).



(a) - 470 x 350 μm    (b) - 470 x 470 μm    (c) - 470 x 470 μm
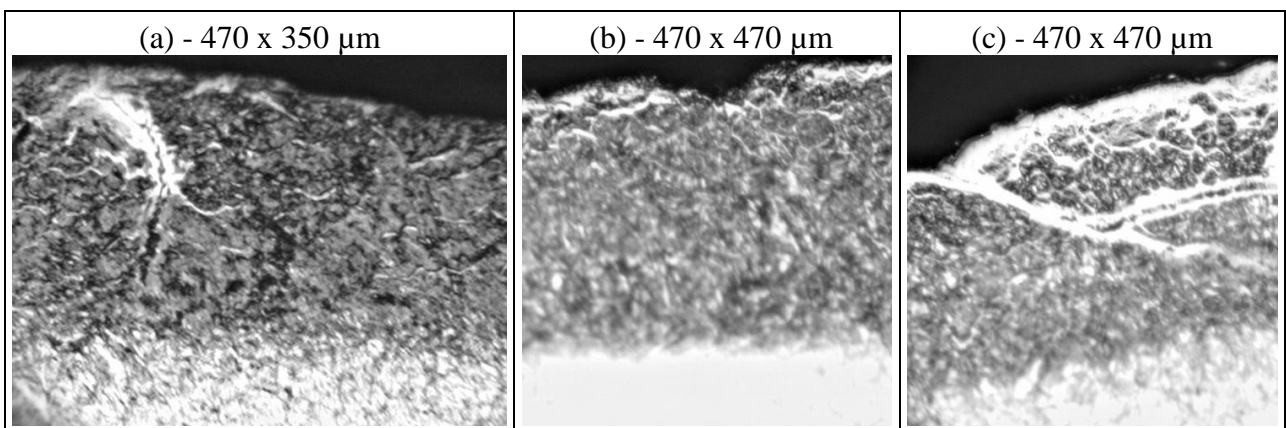
# Tables

Table 1 – Standard compositional limits of the ISO X40CrMoV5-1 steel grade[7].

|      | C    | Si  | Mn   | Cr  | Mo  | V    | P    | S    |
|------|------|-----|------|-----|-----|------|------|------|
| Min. | 0.35 | 0.8 | 0.25 | 4.8 | 1.2 | 0.85 | -    | -    |
| Max. | 0.42 | 1.2 | 0.50 | 5.5 | 1.5 | 1.15 | 0.03 | 0.02 |

Table 2 – Service and nitrocarburizing schedule of the B die. Total and partial press cycles numbers (recorded) and wear lengths (estimated from billet mass and extrudate linear mass), before each nitrocarburizing stage, and before the final examination.

| Press cycle | | Wear length | | Nitrocarburizing |
|-------|---------|-------|---------|-------|
| Total | Partial | Total | Partial | stage |
| #     | #       | km    | km      | #     |
| 5     | 5       | 0.2   | 0.2     | 1     |
| 28    | 23      | 1.2   | 0.9     | -     |

Table 3 – Service and nitrocarburizing schedule of the C die. Same as Table 3, plus service times (including billet-exchange stops) estimated from a 5 h production test. Some initial stages were not recorded in detail.

| Press cycle | | Wear length | | Service time | | Nitrocarburizing |
|---|---|---|---|---|---|---|
| Total | Partial | Total | Partial | Total | Partial | stage |
| # | # | km | km | h | h | # |
| 246 | n. a. | 11.7 | n. a. | 9.7 | n. a. | 4 |
| 348 | 102 | 16.5 | 4.8 | 13.7 | 4.0 | 5 |
| 426 | 78 | 20.2 | 3.7 | 16.7 | 3.1 | 6 |
| 469 | 43 | 22.2 | 2.0 | 18.4 | 1.7 | 7 |
| 497 | 28 | 23.6 | 1.3 | 19.5 | 1.1 | 8 |
| 583 | 86 | 27.7 | 4.1 | 22.9 | 3.4 | 9 |
| 679 | 96 | 32.2 | 4.6 | 26.7 | 3.8 | 10 |
| 798 | 119 | 37.8 | 5.6 | 31.4 | 4.7 | 11 |
| 905 | 107 | 42.9 | 5.1 | 35.6 | 4.2 | 12 |
| 1060 | 155 | 50.3 | 7.4 | 41.7 | 6.1 | - |

Table 4 - Standard compositional limits of the 6060 aluminium alloy[31].

|       | Mg   | Si  | Fe  | Mn  | Zn   | Cu  | Cr   | Ti  |
|-------|------|-----|-----|-----|------|-----|------|-----|
| Min.  | 0.35 | 0.3 | 0.1 | -   | -    | -   | -    | -   |
| Max.  | 0.6  | 0.6 | 0.3 | 0.1 | 0.15 | 0.1 | 0.05 | 0.1 |

Table 5 – Typical composition of the employed nitrocarburizing salt bath[14].

| $CN^-$  | $CNO^-$  | $CO_3^{2-}$ | $K^+$     | $Na^+$   | $Li^+$       | $S^{2-}$  |
|---------|----------|-------------|-----------|----------|--------------|-----------|
| ≤0,8 %  | 36±2 %   | 19±2 %      | 24,5±2 %  | 20±2 %   | 1,25±0,2 %   | 2-10 ppm  |